Controlling the Coulomb Explosion of Silver Clusters by Femtosecond Dual-Pulse Laser Excitation

T. Döppner,* Th. Fennel,† Th. Diederich, J. Tiggesbäumker, and K. H. Meiwes-Broer
Institut für Physik, Universität Rostock, 18051 Rostock, Germany
(Received 13 August 2004; published 6 January 2005)

Silver clusters grown in helium nanodroplets are excited by intense femtosecond laser pulses resulting in the formation of a hot electron plasma far from equilibrium. The ultrafast dynamics is studied by applying optically delayed dual pulses, which allows us to pursue and control the coupling of the laser field to the clusters on a femtosecond time scale. A distinct influence of the optical delay on the ionization efficiency gives strong evidence that a significant contribution of collective dipolar electron motion is present, which is verified by corresponding Vlasov dynamics simulations on a model system. The microscopic approach demonstrates the outstanding role of giant resonances in clusters also in intense laser fields.

DOI: 10.1103/PhysRevLett.94.013401 PACS numbers: 36.40.Gk, 52.50.Jm, 52.65.Rr

The fascinating results from the interaction of intense femtosecond (fs) light pulses with clusters are nanometer-sized highly nonstationary plasmas. The efficient absorption of laser radiation by clusters is reflected in the generation of highly charged ions with 10^5–10^6 eV kinetic energy [1,2], x-ray emission [3], and even fusion events [4]. Recently, the research in this field was intensified by the need for novel intense ultraviolet and x-ray sources, e.g., for extreme ultraviolet lithography [5–7]. Besides technological relevance the fundamental problem of the interaction of ultrashort and intense laser fields with matter on the nanometer scale is still under study. Even though there is evidence from both experimental and theoretical work that collective electron excitations dominate the coupling process between laser pulses and clusters [1,2,8–10], details of the electron and ion dynamics have not been resolved yet. So far mainly the technique of pulse stretching was applied. By tuning the pulse width, the charging [9,11] and the x-ray emission [5,6] could be optimized. Numerical simulations have been performed [8,10,12–14] which support the strong contribution by collective electron excitations, though other mechanisms like, e.g., enhanced ionization as observed for molecules [15] or ionization ignition [16], might apply as well in some cases.

In this Letter we pursue a way to resolve the electron and ion dynamics of clusters exposed to intense laser fields in more detail. Following the powerful concept of the pump-probe technique, as, for example, has already been applied for silver nanoparticles in glass matrices [17], a dual-pulse excitation scheme is implemented. With a corresponding fs laser experiment and Vlasov simulations it is shown that both the ''preparation'' and the violent charging of the clusters can independently be considered. The first laser pulse provides the initial ionization which is dominated by nonresonant effects, i.e., tunneling and optical field ionization. This activation step triggers the cluster expansion leading to a redshift of the collective electron modes. The absorption efficiency of the second pulse then depends on the time-dependent optical properties of the expanding system. For a certain optical delay the collective dipolar mode is resonantly excited, resulting in an effective charging of the cluster. Corresponding numerical simulations reveal that the phase relation between the driving laser field and electron motion exhibits a clear $\pi/2$ transition, analogous to a driven harmonic oscillator.

The atom pickup method is used to grow clusters inside superfluid helium droplets [18]. Main parts of the apparatus were designed and constructed by Toennies and his group [19]. A beam of helium nanodroplets is produced by means of a supersonic expansion of pure helium gas at a stagnation pressure of 20 bars through a 5 μm nozzle which can be cooled down to 8.0 K. Under these conditions the droplets consist of up to 10^7 helium atoms. In the pickup chamber metal atoms are successively loaded into the droplets and form clusters. Operating the source with silver, up to 150 atoms aggregate in a single droplet [20]. For excitation, a Ti:sapphire chirped pulse amplification system delivers laser pulses at $\omega_L = 800$ nm (1.54 eV), with a pulse width of 130 fs. In order to achieve double pulses with an adjustable optical delay, a Mach-Zehnder interferometer setup is used. The laser light with a typical energy of 2.5 mJ per pulse, perpendicularly propagating to the cluster beam, is focused by a $f = 1/40$ lens. An adjustment of the laser intensity is usually accomplished by shifting the laser focus with respect to the molecular beam axis. The resulting products of the cluster explosion are detected by a high resolution time-of-flight mass spectrometer. Upon excitation the embedded silver clusters disintegrate, leading to richly structured fragment spectra; see Fig. 1. Besides highly charged atomic Ag^{z+} ions from the Coulomb explosion, singly and doubly charged helium ions, helium cluster ions, and snowball complexes Ag^+He_N with $N \leq 150$ are detected. Such spectra are recorded for each optical delay, and those channels of the

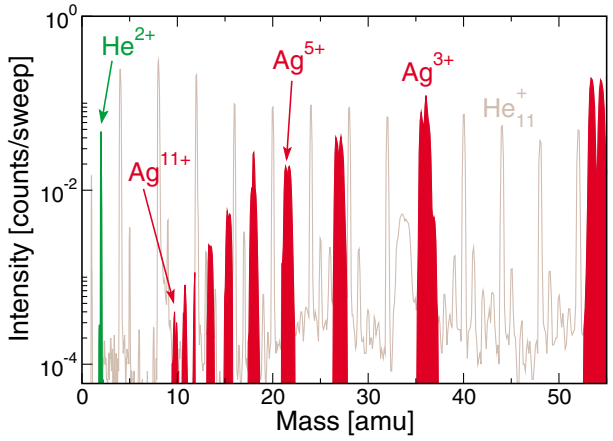

FIG. 1 (color online). Fragment spectrum of silver clusters with a mean number of atoms $N = 40$ in helium droplets exposed to $\omega_L = 800$ nm (1.54 eV) fs laser radiation at 4×10^{13} W/cm^2. The resulting Ag^{z+} signals are highlighted. In this example the charge distribution reaches up to $z = 11$.

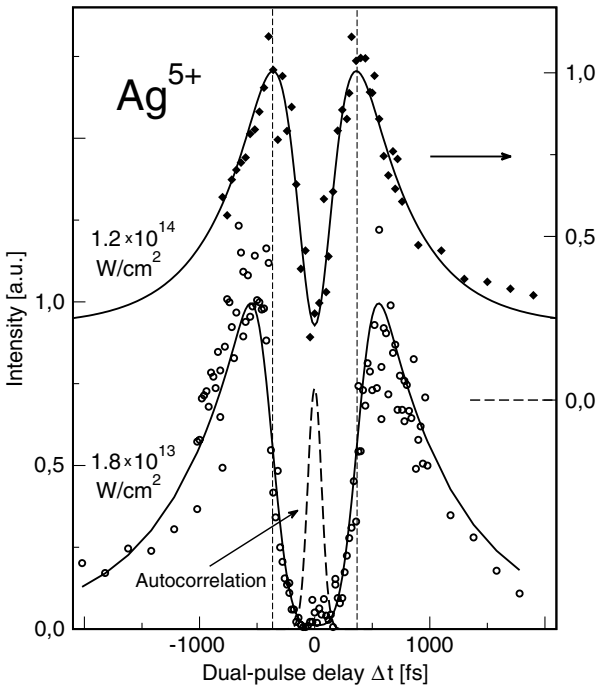

FIG. 2. Normalized dual-pulse signals for Ag^{5+} from the Coulomb explosion of silver clusters in helium droplets, resulting from the excitation with 130 fs pulses. The autocorrelation function is given for comparison. Negative delays correspond to a reversal of the two pulses. The signal at higher intensity was shifted by an offset (see right axis). Data points are fitted using a function that is symmetric with respect to zero delay in order to account for identical laser pulses (solid lines). The peak positions shift to a shorter delay when a higher laser intensity is applied (see dashed vertical lines for comparison).

spectrum that can be assigned to a certain charge state are integrated and analyzed. Similar ionization efficiency profiles are observed for all ionic charge states. As a typical example, Fig. 2 demonstrates the outcome of a dual-pulse experiment with the signals of the Ag^{5+} ion for two different laser intensities. The delay spectra show common characteristics: optical delays close to zero yield only a low ionization signal. This is in contrast to atoms, where the ionization strongly depends on the laser intensity and an enhanced signal would be expected when both pulses overlap. With increasing delay the dual-pulse signal rises strongly to a distinct maximum and decreases nearly exponentially beyond. The value of Δt at the maximum signal defines an optimal delay Δt_{opt} for the most efficient generation of the particular charge state z. At the higher laser intensity this peak position shifts towards a shorter delay; see Fig. 2. Plotting $\Delta t_{\mathrm{opt}}(z)$ at a given laser intensity up to the highest observed charge state z_{max}, we obtain a convergence towards $\Delta t_{\mathrm{opt}}(z_{\mathrm{max}})$. An analysis for the intensities corresponding to the data in Fig. 2 yields values of $\Delta t_{\mathrm{opt}}(z_{\mathrm{max}}) = 550$ and 260 fs for 1.8×10^{13} and 1.2×10^{14} W/cm^2, respectively. Generally, for stronger laser fields the charge distributions extend to higher z values.

The experimental results on Ag_N are in qualitative agreement with sequential steps of activation and resonant ionization as introduced above. Whereas the general trends can readily be understood, the contribution of the collective electron excitation has to be considered in more detail. Therefore we have theoretically investigated the time-dependent response of metal clusters for ultrashort and intense dual-pulse excitation. As a convenient method for the description of violent excitations, the Thomas-Fermi-Vlasov molecular dynamics (TFV-MD) was applied as described in detail in Ref. [21]. TFV-MD provides a semiclassical treatment of the electrons linked to classical dynamics for the ions, close to time-dependent local density approximation [22]. In order to keep the simulations numerically feasible, sodium clusters are chosen as model systems. These are well tested prototypes for simple metal clusters [14,21]. For the interaction between valence electrons and ions a local pseudopotential is adequate to describe the nucleus and the frozen core electrons. Since the number of active electrons per atom is limited to one, no higher charges of the atomic cluster components can be predicted from the model. Despite this limitation, the scheme provides a detailed qualitative analysis of the main coupling mechanisms. We present results for Na_{55}, which has a ground state dipole resonance at an energy of $\hbar\omega_0 = 2.84$ eV within the semiclassical model [21]. In the simulations the clusters are exposed to laser intensities of up to 8×10^{12} W/cm^2. The dual laser pulses are described as linearly polarized dipole fields with a Gaussian pulse envelope having a width of 50 fs, using the experimental photon energy of $\hbar\omega_L = 1.54$ eV. Results from a selected simulation run are shown in Fig. 3 for a pulse delay of 250 fs. During the interaction with the first pulse only, the dipole response signal shown in Fig. 3(a) is weak as the resonance is still far away from the photon energy of the laser, expressed by a dipole phase angle close to zero,

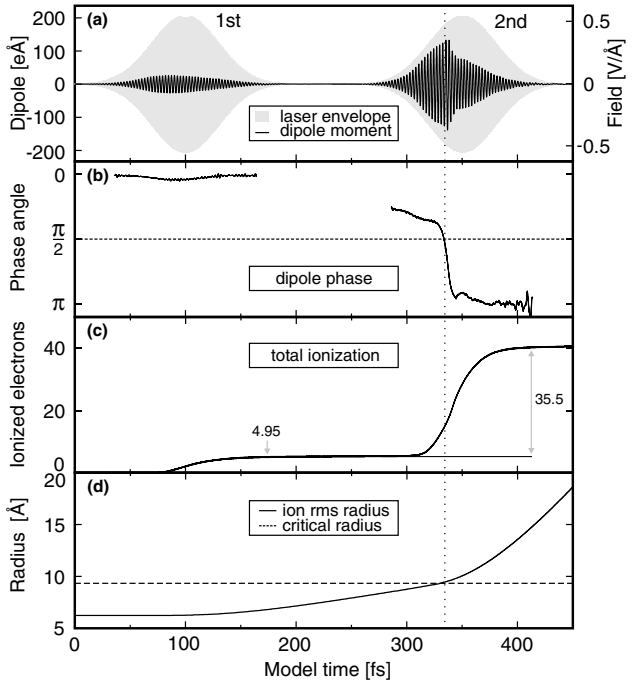

FIG. 3. Response of Na_{55} for dual-pulse excitation with $I = 4 \times 10^{12}$ W/cm^2, $\hbar\omega_L = 1.54$ eV, and an optical delay of 250 fs. (a) The envelope of the laser field (gray) and the corresponding electron dipole amplitude, (b) the phase angle between the laser field and the dipole signal, (c) the total cluster ionization, and (d) the root-mean-square radius of the ion distribution. Note that the dipole phase angle passes $\pi/2$ as the rms radius is close to the critical value R_c (dotted vertical line).

Fig. 3(b). As a result of this off-resonant activation, about five electrons are removed due to field ionization, leaving the cluster in a preionized excited state, Fig. 3(c). The activated cluster now expands as can be seen from the increasing rms radius in Fig. 3(d) leading to a steady decrease of the collective resonance energy. An enhanced optical absorption is expected when the resonance matches the photon energy of the driving laser field which occurs at a critical radius R_c. A rough estimate can be obtained from the Mie formula to be $R_c = R_0(\omega_0/\omega_L)^{2/3}$ with R_0 the initial cluster radius. For Na_{55} this yields a value of about $1.5R_0$, indicated as a dashed line in Fig. 3(d). When applying the second pulse at that particular optical delay, the dipole signal is strongly enhanced compared to the first pulse, indicating violent collective oscillation. Moreover, the phase angle passes through a value of $\pi/2$ when the dipole amplitude is at its maximum leading to a most efficient energy absorption at about 335 fs, in analogy to a classical damped oscillator. The effect on the ionization is shown in Fig. 3(c). About 35 electrons escape due to the second pulse, while only five electrons were removed by the first one. Since the pulses are identical, the huge difference in the ionization efficiency obviously originates from the energy shift of the dipole resonance during expansion. Eventually the cluster decays in a Coulomb explosion caused by the 40-fold ionization of the system.

To further simulate the experimental situation we now vary the pulse delay. The average atomic ionization of the cluster serves as a measure for the coupling efficiency, as shown in Fig. 4. Obviously for all laser intensities investigated the ionization signals exhibit clear maxima. With increasing laser intensity these peaks shift to shorter delay times, in accordance with the experimental findings; see Fig. 2. This results from a faster expansion due to the more intense activation by the first pulse, while the total ionization is rising because of the more violent action of the second pulse. The important role of the giant dipole resonance for the interaction between the cluster and the laser field can be demonstrated with a nonintuitive phenomenon. At a constant optical delay, e.g., of $\Delta t = 300$ fs, a *dropping* ionization efficiency is predicted when *increasing* the laser power within the studied intensity range; see Fig. 4. In fact, this apparent contradiction can be experimentally worked out.

Even though the Vlasov model is limited with respect to the degree of ionization, it allows for a detailed interpretation of the experimental results for Ag_N. The simulations reproduce the main features of the measurements, except

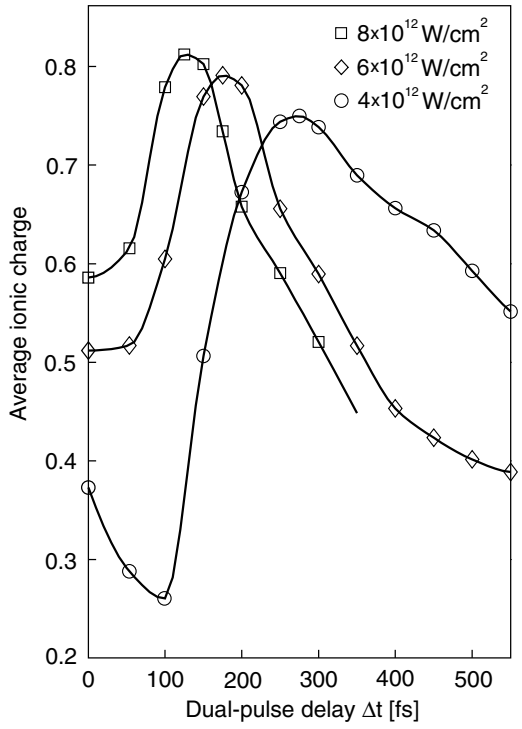

FIG. 4. Calculated average ionic charge after dual-pulse excitation of the model system Na_{55} as a function of the optical delay. Both pulses have a width of 50 fs at the intensities given in the figure. All ionization profiles show a strong delay dependence with a distinct peak. For overlapping pulses the constructive interference leads to a higher effective field strength which explains the signal enhancement at short delays for the lowest intensity.

for the time scale. However, this deviation can be well explained by the characteristics of the particular system. The atomic mass ratio of $m_{Ag}/m_{Na} \approx 5$ decelerates the cluster expansion in silver. Moreover, the higher ground state dipole resonance energy of Ag_N requires a larger relative expansion to match the critical radius R_c. Thus the time delay that is necessary to meet the resonance condition is longer compared to the sodium model system.

Finally, we have to consider the possible influence of the helium droplets encapsulating the silver clusters. With molecular dynamics simulations it can be shown that the surrounding helium causes no significant deceleration of the exploding metal cluster. Second, for the laser intensities used in the experiments, helium can be considered to be almost transparent, as the field ionization threshold is as high as 10^{15} W/cm^2. Hence only a minor dielectric amplification of the local field at the cluster-helium interface is expected. Only at a significantly higher laser intensity can helium actively contribute to the charging dynamics.

In conclusion, the application of fs dual pulses proved to be a powerful technique to investigate and control the charging dynamics of clusters in intense laser fields. Compared to the previously used method of stretching single laser pulses, the dual-pulse signals show a substantially enhanced ionization dynamics with high time resolution. We demonstrate that the initial and the resonant ionization can be treated separately. As a rule of thumb, it can be stated that the laser intensity of the first pulse defines the time delay for highest charging, whereas the second one determines the magnitude of the ionization signal. The overall profile of the dual-pulse signals, the pulse delay for optimized ionization yield, as well as their intensity dependence are in qualitative agreement with the results from the microscopic model. It turns out that resonant enhanced ionization is effective even for laser photon energies far below the ground state dipole resonance. The double pulse technique is a step towards a controlled production of charge-state selected ions, with the corresponding consequences for efficient light generation at desired wavelengths. Further control is to be expected with the application of pulses, which are shaped in the time domain.

We thank J. P. Toennies for providing us with the helium droplet technology. Support by the Max-Planck-Gesellschaft as well as financial aid by the Deutsche Forschungsgemeinschaft within the Sonderforschungsbereich SFB 198 and the Graduiertenkolleg 567 are gratefully acknowledged. Computational resources have been provided by the *Verbund für Hoch- und Höchstleistungsrechnen Nord* (HLRN).

*Corresponding author.
Electronic address: tilo.doeppner@uni-rostock.de

†Corresponding author.
Electronic address: thomas.fennel@uni-rostock.de

[1] T. Ditmire, E. Springate, J. W. G. Tisch, Y. L. Shao, M. B. Mason, N. Hay, J. P. Marangos, and M. H. R. Hutchinson, Phys. Rev. A **57**, 369 (1998).
[2] S. Teuber, T. Döppner, T. Fennel, J. Tiggesbäumker, and K. H. Meiwes-Broer, Eur. Phys. J. D **16**, 59 (2001).
[3] A. McPherson, B. D. Thompson, A. B. Borisov, K. Boyer, and C. K. Rhodes, Nature (London) **370**, 631 (1994).
[4] T. Ditmire, J. Zweiback, V. P. Yanovsky, T. E. Cowan, G. Hays, and K. B. Wharton, Nature (London) **398**, 489 (1999).
[5] E. Parra, I. Alexeev, J. Fan, K. Y. Kim, S. J. McNaught, and H. M. Milchberg, Phys. Rev. E **62**, R5931 (2000).
[6] M. Schnürer, S. Ter-Avetisyan, H. Stiel, U. Vogt, W. Radloff, M. Kalashnikov, W. Sandner, and P. V. Nickles, Eur. Phys. J. D **14**, 331 (2001).
[7] S. Düsterer, H. Schwoerer, W. Ziegler, D. Salzmann, and R. Sauerbrey, Appl. Phys. B **76**, 17 (2003).
[8] T. Ditmire, T. Donnelly, A. M. Rubenchik, R. W. Falcone, and M. D. Perry, Phys. Rev. A **53**, 3379 (1996).
[9] L. Köller, M. Schumacher, J. Köhn, S. Teuber, J. Tiggesbäumker, and K.-H. Meiwes-Broer, Phys. Rev. Lett. **82**, 3783 (1999).
[10] U. Saalmann and J.-M. Rost, Phys. Rev. Lett. **91**, 223401 (2003).
[11] E. Springate, N. Hay, J. W. G. Tisch, M. B. Mason, T. Ditmire, M. H. R. Hutchinson, and J. P. Marangos, Phys. Rev. A **61**, 063201 (2000); V. Kumarappan, M. Krishnamurthy, and D. Mathur, Phys. Rev. A **66**, 033203 (2002); M. A. Lebeault, J. Viallon, J. Chevaleyre, C. Ellert, D. Normand, M. Schmidt, O. Sublemontier, C. Guet, and B. Huber, Eur. Phys. J. D **20**, 233 (2002).
[12] K. Andrae, P.-G. Reinhard, and E. Suraud, Phys. Rev. Lett. **92**, 173402 (2004); K. Andrae, P.-G. Reinhard, and E. Suraud, J. Phys. B **35**, 4203 (2002).
[13] T. Döppner, S. Teuber, M. Schumacher, J. Tiggesbäumker, and K. H. Meiwes-Broer, Appl. Phys. B **71**, 357 (2000).
[14] J. Daligault and C. Guet, Phys. Rev. A **64**, 043203 (2001).
[15] T. Zuo and A. D. Bandrauk, Phys. Rev. A **52**, R2511 (1995); T. Seideman, M. Yu. Ivanov, and P. B. Corkum, Phys. Rev. Lett. **75**, 2819 (1995); Ch. Siedschlag and J.-M. Rost, Phys. Rev. A **67**, 013404 (2003).
[16] C. Rose-Petruck, K. J. Schäfer, K. R. Wilson, and C. P. J. Barty, Phys. Rev. A **55**, 1182 (1997); K. Ishikawa and T. Blenski, Phys. Rev. A **62**, 063204 (2000).
[17] M. Perner, S. Gresillon, J. März, G. von Plessen, J. Feldmann, J. Porstendorfer, K.-J. Berg, and G. Berg, Phys. Rev. Lett. **85**, 792 (2000).
[18] Special edition on helium nanodroplets [J. Chem. Phys. **115**, 10 065 (2001)].
[19] A. Bartelt, J. D. Close, F. Federmann, N. Quaas, and J. P. Toennies, Phys. Rev. Lett. **77**, 3525 (1996).
[20] P. Radcliffe, A. Przystawik, Th. Diederich, T. Döppner, J. Tiggesbäumker, and K. H. Meiwes-Broer, Phys. Rev. Lett. **92**, 173403 (2004).
[21] Th. Fennel, G. F. Bertsch, and K. H. Meiwes-Broer, Eur. Phys. J. D **29**, 367 (2004).
[22] L. Plagne, J. Daligault, K. Yabana, T. Tazawa, Y. Abe, and C. Guet, Phys. Rev. A **61**, 033201 (2000).